Excited-State Dynamics of 12′-Apo-β-caroten-12′-al and 8′-Apo-β-caroten-8′-al in Supercritical CO_2, N_2O, and CF_3H

Florian Ehlers,[†] Thomas Lenzer,*[,†,‡] and Kawon Oum*[,†,‡]

Max-Planck-Institut für biophysikalische Chemie, Abt. Spektroskopie und Photochemische Kinetik (10100), Am Fassberg 11, 37077 Göttingen, Germany, and Georg-August-Universität Göttingen, Institut für Physikalische Chemie, Tammannstrasse 6, 37077 Göttingen, Germany

Received: August 8, 2008; Revised Manuscript Received: October 18, 2008

The ultrafast excited-state dynamics of the two carbonyl carotenoids 12′-apo-β-caroten-12′-al (12′C) and 8′-apo-β-caroten-8′-al (8′C) have been investigated in supercritical (sc) fluids by femtosecond transient absorption spectroscopy. CO_2, N_2O, and CF_3H were employed as solvent media over the pressure range 85−300 bar and at the temperatures 308 and 323 K. The carotenoids were excited to the S_2 state at 390 nm, and the subsequent dynamics were probed at different wavelengths in the UV−vis (390, 545, 580, 600, and 650 nm) and near IR (780 nm) regions. Stimulated emission in the near IR signaled the presence of a state with intramolecular charge transfer character (S_1/ICT). For 12′C in scCO_2 and scN_2O, the internal conversion (IC) time constant τ_1 for the S_1/ICT → S_0 transition showed no systematic pressure dependence and yielded an average value of 190 ps. This is slightly smaller than the values in nonpolar organic solvents (ca. 220 ps) found in our previous studies and probably due to the substantial quadrupole moment of the nondipolar CO_2 and the small dipole moment of N_2O, which might slightly stabilize the S_1/ICT state relative to S_0. This results in an acceleration of the nonradiative rate in the simple framework of an energy gap law approach. In polar CF_3H, a pronounced acceleration of the internal conversion rate was observed with increasing pressure, which can be explained by the polarity increase, as characterized by the parameter $\Delta f = (\varepsilon - 1)/(\varepsilon + 2) - (n^2 - 1)/(n^2 + 2)$. We find sc$CF_3H$ to be the first solvent where the S_1/ICT state of 12′C does not decay in a monoexponential fashion. This is most likely attributed to time-dependent solvation of the S_1/ICT state, vibrational cooling, or conformational relaxation processes in 12′C. In addition, we studied the dynamics of the longer conjugated species 8′C, where the decays of all transients in scCO_2 and scCF_3H could be described well by monoexponential fits, in good agreement with previous results in organic solvents. Anisotropy decays from polarization spectroscopy of the 12′C species provided orientational relaxation time constants which were increasing with viscosity. The values in scCO_2 were extrapolated to a free rotor time of 4.6 ps, which is in good agreement with a value of 5.2 ps calculated on the basis of the rotational constants. We also report on pressure- and temperature-dependent steady-state absorption spectra of the two apocarotenals in scCO_2, scN_2O, and scCF_3H. The band position of the S_0 → S_2 transition correlates well with solvent polarizability, but—in contrast to our previous study of C_{40} carotenoids—a substantial influence of polarity was also observed. Specifically, we found indications for solvent clustering, resulting in a saturation of the solvent shift at lower densities.

1. Introduction

Knowledge of the energetics and relaxation of carotenoid excited electronic states and their dependence on conjugation length, the presence of substituents, isomeric structure, and solvent environment is a prerequisite for understanding the interactions and dynamics of carotenoids involved in photobiology.[1,2] In this report, we are focused on employing the special solvent properties of supercritical fluids (SCFs) for investigating carotenoid species. Some of the unique features that characterize SCFs are liquid-like densities and solubilities and gas-like viscosities and diffusivities which are intermediate between typical gas and liquid values.[3] The most important feature of a supercritical fluid is the tunability of its physical properties without changing the chemical nature of the solvent. Thus, solvent properties such as density, diffusivity, capacity for solutes, viscosity, refractive index, and dielectric constant can be easily and continuously changed by the use of SCFs simply by adjusting temperature and pressure.[4−14] Specifically, much lower solvent polarizabilities can be reached in SCFs compared to standard organic solvents, allowing, e.g., to shift the electronic S_0 → S_2 transition of carotenoids to higher energies not accessible by conventional solvents. Such a strategy, for instance, enabled reliable extrapolations of the S_0 → S_2 0−0 transition of several C_{40} carotenoids toward the gas-phase limit.[5]

The fluids used in this work are CO_2, N_2O, and CF_3H. These were chosen because they are most commonly used in supercritical fluids science and technology, covering a broad range of properties (e.g., dielectric constants and polarizabilities), and their critical regions are easy to access experimentally. Critical constants are the following: for CO_2, critical temperature (T_c) = 304.18 K, critical pressure (P_c) = 73.77 bar, and critical density (ρ_c) = 0.4676 g/mL; for N_2O, T_c = 309.52 K, P_c = 72.45 bar, and ρ_c = 0.4520 g/mL; for CF_3H, T_c = 299.29 K, p_c = 48.32 bar, and ρ_c = 0.5270 g/mL.[15] Values of the refractive

* E-mail: koum@gwdg.de. Fax: +49 551 39 3150. Phone: +49 551 39 12598.
[†] Max-Planck-Institut für biophysikalische Chemie.
[‡] Georg-August-Universität Göttingen.

10.1021/jp807086n CCC: $40.75
Published on Web 11/21/2008

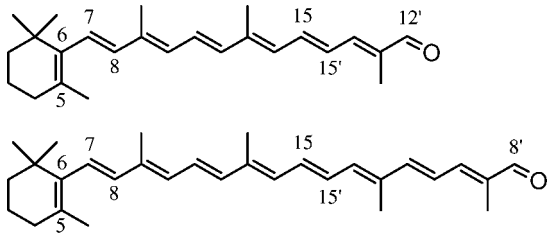

Figure 1. Structures of 12′-apo-β-caroten-12′-al (12′C, top) and 8′-apo-β-caroten-8′-al (8′C, bottom).

index (n) and dielectric constant (ε) needed for the analysis of solvatochromic shifts and polarity of supercritical CO_2 and CF_3H were obtained from the analytical forms suggested by Maroncelli and co-workers:[11]

For CO_2:

$$R(n) = \frac{n^2 - 1}{n^2 + 2} = 0.07016\rho_r + 1.412 \times 10^{-4}\rho_r^2 - 3.171 \times 10^{-4}\rho_r^3 \quad (1)$$

$$\varepsilon - 1 = 0.2386\rho_r + 0.02602\rho_r^2$$

For CF_3H:

$$R(n) = \frac{n^2 - 1}{n^2 + 2} = 0.05374\rho_r - 3.136 \times 10^{-4}\rho_r^2 - 1.534 \times 10^{-4}\rho_r^3 \quad (2)$$

$$R(\varepsilon) = \frac{\varepsilon - 1}{\varepsilon + 2} = 0.1723\rho_r + 100.6\left(\frac{\rho_r}{T}\right)\exp(-0.1530\rho_r^2)$$

Here, ρ_r is the reduced density of the fluids and T is the temperature in Kelvin; the Lorentz−Lorenz function $R(n) = (n^2 - 1)/(n^2 + 2)$ represents the solvent polarizability, and the reaction field factor $R(\varepsilon) = (\varepsilon - 1)/(\varepsilon + 2)$ considers permanent and induced dipole contributions. Solvent dipolarity can be estimated by the Δf scale:

$$\Delta f = R(\varepsilon) - R(n) = \frac{\varepsilon - 1}{\varepsilon + 2} - \frac{n^2 - 1}{n^2 + 2} \quad (3)$$

For instance, the resulting density dependence of Δf values of supercritical CO_2 and CF_3H is in the range of 0.01−0.02 and 0.44−0.60, respectively, for the density range employed in the time-resolved experiments of the present study. On the basis of the Δf scale, supercritical CO_2 is a nondipolar solvent (however, having a considerable quadrupole moment),[16] whereas supercritical CF_3H is a medium-polar solvent with Δf values lying between tetrahydrofuran (0.44) and acetone (0.65).

In this work, we investigated the ultrafast excited-state dynamics of the carbonyl substituted carotenoids 12′C and 8′C in supercritical CO_2, N_2O, and CF_3H over the pressure range 85−300 bar at $T = 308$ and 323 K and compared the results with those previously obtained in organic solvents.[17−19] The chemical structures of both apocarotenals are shown in Figure 1. The 12′C species is of particular interest, because we previously found a pronounced polarity dependence of the lifetime τ_1 of its first electronically excited state ("S_1/ICT"), varying between 220 ps in n-hexane and 8 ps in methanol, which correlated well with the polarity parameter Δf.[18] The current measurements in SCFs are intended to test the validity of this correlation and provide additional information on specific solvation effects of carotenoids in SCFs.[11,12]

In addition, we present for the first time density-dependent orientational relaxation times of carotenoids in SCFs, which—due to the very low viscosity range covered by these fluids (down to 0.03 cP in the current experiments)—enables a meaningful extrapolation to the free rotor limit. So far, studies of β-carotene using resonance enhanced optical Kerr effect spectroscopy have focused on a series of n-alkanes with viscosities >0.234 cP,[20,21] which are much higher than those accessible in the current study using SCFs. In such studies, besides viscosity, also the molecular structure and shape of the solvent are varied which make the interpretation of the results more complicated.[22]

We also report on density- and temperature-dependent steady-state absorption spectra for the $S_0 \rightarrow S_2$ transition of 12′C and 8′C in $scCO_2$, scN_2O, and $scCF_3H$. Because of their terminal carbonyl substitution, the apocarotenals already possess a considerable dipole moment in the electronic ground state in contrast to the symmetric C_{40} carotenoids studied previously by us.[5] This allows us to quantify the relative importance of polarizability- and polarity-related contributions to the static spectral shifts.

2. Experimental Section

The femtosecond UV/vis/NIR transient absorption setup was already described in our previous publications.[17,19,23] Briefly, the apocarotenals were excited near the maximum of the $S_0 \rightarrow S_2$ absorption band by 390 nm laser pulses obtained by frequency-doubling part of the output of a Ti:sapphire oscillator-regenerative amplifier system (780 nm, 1 kHz, 1 mJ pulse^{-1}, 100 fs) in a BBO crystal. For probe beam generation, the 780 nm beam was either used directly or frequency-doubled in a BBO crystal to 390 nm. Alternatively, the fundamental was directed into a home-built blue-pumped two-stage noncollinearly phase-matched optical parametric amplifier (NOPA) to generate the probe wavelengths 545, 580, 600, or 650 nm. The NOPA output was subsequently compressed by a pair of quartz prisms. The wavelengths cover the ground-state bleach ($S_0 \rightarrow S_2$), vis excited-state absorption (S_1/ICT $\rightarrow S_n$), and near IR transient absorption/stimulated emission ($S_2 \rightarrow S_n$, S_1/ICT $\rightarrow S_0$) bands of these molecules.[17−19] The relative delay of the pump and probe pulses was adjusted by a computer-controlled stage. Each beam was attenuated and mildly focused nearly collinearly into a home-built stainless steel high-pressure cell with 2 mm thick sapphire windows and a path length of 1 mm (diameter of the light spot approximately 250 μm). The cell consisted of two halves sealed by a PTFE O-ring. Sapphire windows with their C-axis perpendicular to the window surface were employed to avoid depolarization of the laser beams. This eliminates birefringence effects and prevents changes in the beam polarization.[4] For population relaxation measurements, the relative polarization of the pump and probe beams was adjusted to 54.7° (magic angle) to avoid any contribution from orientational relaxation. Time-dependent anisotropies were determined from additional measurements using parallel and perpendicular relative polarization of the pump and probe beams.

Pulse energies for the pump and probe beams were 2 μJ or less. Probe energies were measured by two photodiodes, which were located in front of and behind the high-pressure cell. A chopper wheel blocked every second pump pulse. The change in optical density (ΔOD) was obtained from the differences of

the optical densities with and without the pump beam. For each delay time, typically 4000−16000 laser shots were averaged. The time resolution of the setup was between 100 and 150 fs. Coherent artifacts were observed for some of the signals, especially at low pressures in CO_2 and N_2O, where the carotenoid signals were small. These spikes were fitted by monoexponential responses convolved with the cross-correlation time and not considered in modeling the population kinetics.

The apocarotenals were first dissolved in a small amount of acetone and pipetted into the reservoir of one of the cell halves. After complete evaporation of the acetone, the cell was assembled and pressurized with a syringe pump using liquid CO_2, N_2O, or CF_3H, which were subsequently heated up to the temperature of interest. The apocarotenal concentration was always kept below its solubility limit ($<10^{-5}$ M). From steady-state absorption measurements, it was determined that the carotenoids completely dissolve in the SCFs under the selected conditions. The pressure was measured by a high-pressure gauge having an accuracy of ±0.01 MPa. The temperature was detected inside the cell using a Pt100 temperature sensor and was controlled within ±0.1 K by a programmable temperature controller. The cell content was efficiently mixed by a magnetic stir bar, which was controlled by an external motor-driven magnet.

Interestingly, in the case of scN_2O, we observed a decay of the signal size in the transient absorption experiments on a time scale of minutes, presumably due to epoxidation reactions at the double bond system[24] or other oxidative degradation reactions.[25] This effect was minimized by recording scans forward and backward in time in an alternate fashion, normalizing the individual scans to the same initial amplitude, and subsequent averaging, which still yielded reliable decay time constants.

The optical high-pressure cell for the quasi-static absorption measurements in supercritical fluids and the loading of this cell with carotenoid samples were already described in ref 5. Absorption spectra were taken using a Varian CARY 5E spectrometer over the wavelength range 200−800 nm at a spectral resolution of 0.1 nm. Each sample spectrum was corrected by the reference spectrum measured in the SCF only. For the steady-state absorption spectra in scN_2O, we did not observe any change in the shape of the spectra despite decomposition. Presumably the decomposition products absorb at much shorter wavelengths because of their shorter conjugation length and therefore do not interfere with the absorption of the apocarotenals in the 320−550 nm region. The highly purified carotenoid samples were generously provided by BASF AG. 12′-Apo-β-caroten-12′-al and 8′-apo-β-caroten-8′-al were all in their *all-trans* (*all-E*) configuration with a purity >97%. The SCFs had purities of ≥99.996% (CO_2, Praxair), ≥99.995% (N_2O, Linde), and ≥99.0% (CF_3H, Gerling Holz & Co.).

3. Results

3.1. Steady-State Absorption Spectra. Static absorption spectra of 12′C and 8′C in supercritical CO_2 and CF_3H are compared with those in *n*-hexane and methanol in Figures 2 and 3, respectively. The strong absorption band in the range 320−550 nm is associated with the $S_0(1^1A_g^-) \rightarrow S_2(1^1B_u^+)$ transition.[17−19] The vibronic structure, absorption maximum, and the full width at half-maximum (fwhm) of the absorption band were found to depend strongly on the solvent properties. For example, the vibronic structure of both apocarotenals is visible in nonpolar solvents as shoulders; however, it disappears in polar solvents. In supercritical CO_2 compared to *n*-hexane, such

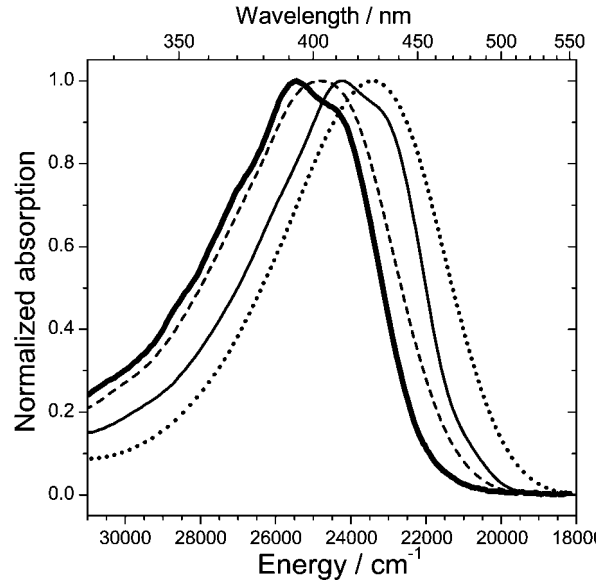

Figure 2. Comparison of steady-state absorption spectra of 12′C in various solvents. From left to right: thick solid line, supercritical CO_2 ($P = 91$ bar, $T = 308$ K, $R(n) = 0.10$); dashed line, supercritical CF_3H ($P = 202$ bar, $T = 308$ K, $R(n) = 0.10$); thin solid line, *n*-hexane ($T = 298$ K, $R(n) = 0.23$); dotted line, methanol ($T = 298$ K, $R(n) = 0.20$). Each spectrum is normalized to the respective absorption maximum.

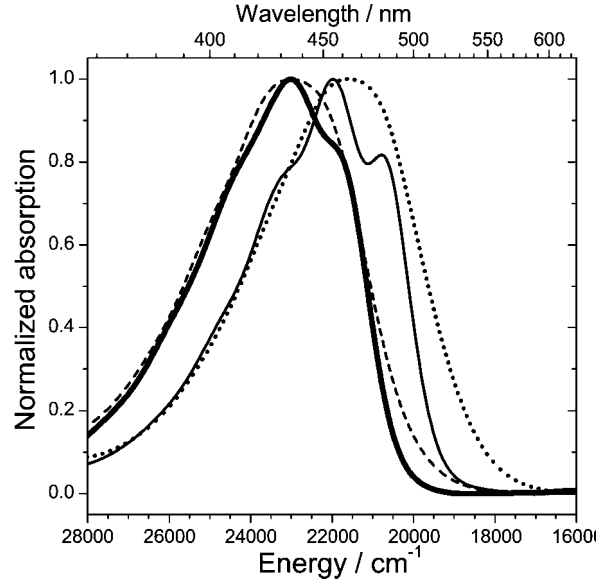

Figure 3. Same as in Figure 2 but for 8′C.

vibronic structure is still observed for 12′C (see Figure 2), while a slightly less structured spectrum was seen for 8′C (see Figure 3). In supercritical CF_3H, both apocarotenals exhibited structureless absorption bands, similar to methanol.

The effect of density change on the absorption maximum of 12′C and 8′C was investigated in supercritical CO_2 and CF_3H over the pressure range 54−301 bar at the two temperatures 308 and 323 K. The absorption maxima and the density-dependent spectra in $scCO_2$ and $scCF_3H$ are summarized in the Supporting Information as Table S1 and Figure S1 for 12′C and Table S2 and Figure S2 for 8′C. In all cases, to higher densities, the position of the main peak of the $S_0(1^1A_g^-) \rightarrow S_2(1^1B_u^+)$ transition exhibited a bathochromic shift by ca. 5−10 nm to longer wavelengths under our experimental conditions.

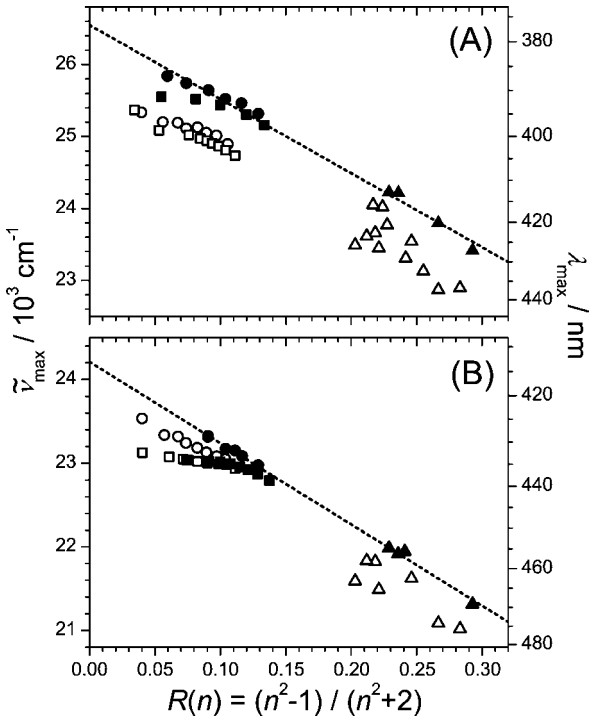

Figure 4. $S_0 \rightarrow S_2$ absorption band maxima of (A) 12′C and (B) 8′C in nonpolar (filled symbols) and polar (open symbols) solvents as a function of solvent polarizability $R(n)$ (for data, see Supporting Information Tables S1 and S2): Supercritical CO_2 at 323 K (●) and 308 K (■), supercritical CF_3H at 323 K (○) and 308 K (□), nonpolar organic solvents (▲), and polar organic solvents (△). Dotted lines are linear fits to the data sets in supercritical CO_2 at 323 K and nonpolar organic solvents (see text).

A considerable hypsochromic spectral shift of the absorption maximum (ca. 20−30 nm) was observed for both apocarotenals in $scCO_2$ and $scCF_3H$ relative to those in *n*-hexane and methanol, respectively. The degree of solvent-induced spectral shifts can be correlated with the Lorentz−Lorenz function $R(n)$: the larger the solvent polarizability, the larger the red shift of the absorption maximum. The $R(n)$ values of organic solvents lie in the range 0.20−0.30, while those of supercritical fluids are much lower, in the range 0.03−0.14,[11] depending on the density of the medium. Figure 4 compares the location of absorption maxima of 12′C and 8′C in various solvents over the respective $R(n)$ range; see the Discussion for details.

The absorption spectra of the 12′C and 8′C species in scN_2O were measured at 323 K over the pressure range 83−301 bar, and the spectral shape and peak position were slightly red-shifted by 3−5 nm relative to $scCO_2$. In the case of scN_2O, density-dependent $R(n)$ values for our experimental conditions are, unfortunately, not yet available and therefore the results cannot be included in Figure 4.

3.2. Transient Absorption Signals. ***3.2.1. 12′-Apo-β-caroten-12′-al.*** The ultrafast excited-state dynamics of 12′C were investigated in the supercritical fluids CO_2, CF_3H, and N_2O, at pressures between 85 and 300 bar and at the temperatures 323 K, 308 K ($scCO_2$, scN_2O, $scCF_3H$), and 296 K (liquid CF_3H). 12′C was excited at 390 nm close to the absorption maximum of the $S_0 \rightarrow S_2$ transition. The excited-state dynamics were probed at different wavelengths covering the $S_0 \rightarrow S_2$ ground-state bleach (GSB: 390 nm) and S_1/ICT $\rightarrow S_n$ excited-state absorption (ESA: 545, 580, 600, and 650 nm). A few measurements were also carried out at the probe wavelength 780 nm to investigate if characteristic stimulated emission (SE) was present in SCFs, which would be a signature of ICT character.[18,26,27]

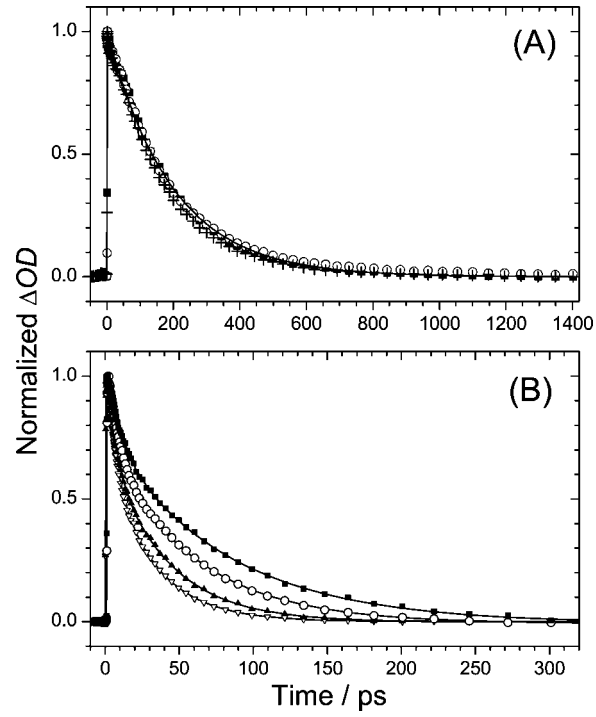

Figure 5. Typical pressure-dependent transient absorption signals of 12′C at 323 K in supercritical CO_2 and CF_3H at different pressures. (A) In $scCO_2$: (■) 125 bar; (○) 200 bar; (+) 300 bar. (B) In $scCF_3H$: (■) 85 bar; (○) 125 bar; (▲) 200 bar; (▽) 300 bar. λ_{pump} = 390 nm, λ_{probe} = 545 nm. The lines represent the best fits described in the text. For fit parameters, see Supporting Information Table S3.

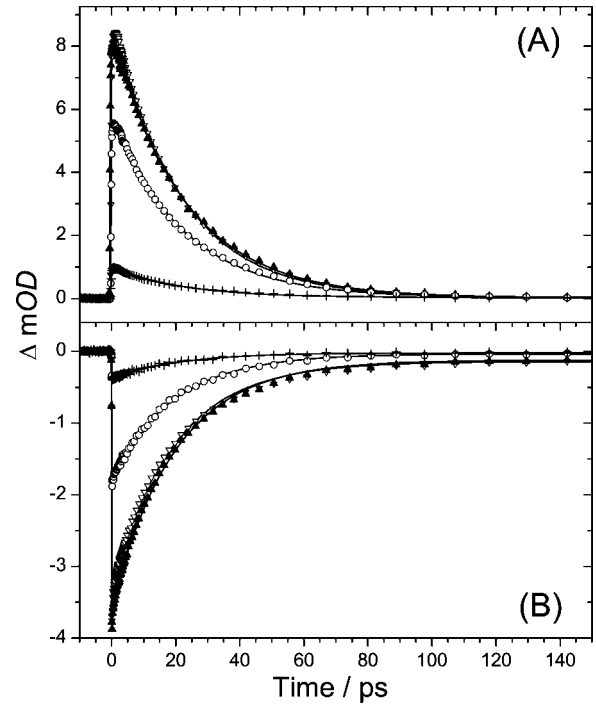

Figure 6. Typical pressure-dependent transient absorption signals of 8′C in supercritical CF_3H at 323 K for two different probe wavelengths: (A) λ_{probe} = 545 nm; (B) λ_{probe} = 390 nm. Different symbols indicate different pressures: (+) 85 bar; (○) 125 bar; (▲) 200 bar; (▽) 300 bar. λ_{pump} = 390 nm. The lines represent the best fits described in the text. For fit parameters, see Supporting Information Table S4.

Figure 5 shows characteristic normalized transient ESA signals (S_1/ICT $\rightarrow S_n$) at 545 nm of 12′C in supercritical CO_2 (A) and CF_3H (B) at different densities over the pressure range

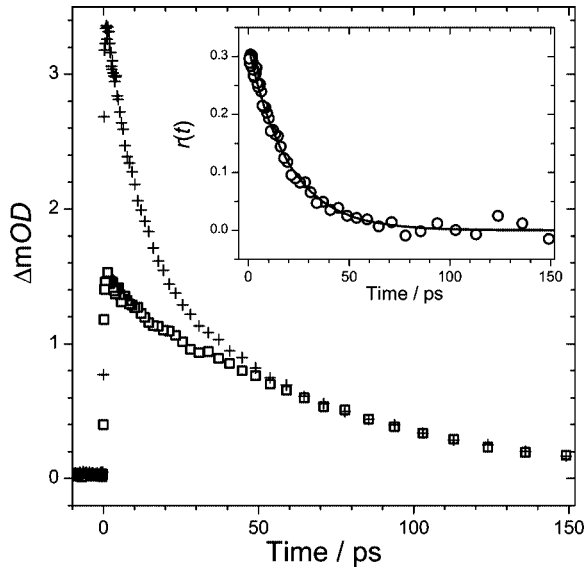

Figure 7. Laser polarization dependence of transient absorption signals of 12′C in supercritical CF_3H at 100 bar and 323 K. Relative polarization between pump and probe beams: (+) parallel; (□) perpendicular. Inset: (○) anisotropy $r(t)$. The line represents a monoexponential fit to the data over the time range 1.3−150 ps. λ_{pump} = 390 nm, and λ_{probe} = 545 nm. For details, see the text.

85−300 bar at 323 K. The signals were fitted by a sum of up to three exponential functions, and representative examples are included in Figure 5. In this paper, we are mainly concerned with the final well-separated decay of the signals which is due to internal conversion from the S_1/ICT state to S_0; for further details of the fitting functions and kinetic parameters, see the Discussion. Supporting Information Table S3 summarizes all experimental conditions and the measured time constants.

The kinetics of the final transient absorption decay of 12′C showed a strong dependence on the solvent environment. In supercritical CO_2, the time constant τ_1 for this decay was in the range 180−220 ps and therefore only weakly changing (see Figure 5A). This was also observed for the other probe wavelength 390 nm, located on the $S_0 \rightarrow S_2$ absorption band. In addition, we employed supercritical N_2O, and found that the decay time constants and density dependence were very similar to those observed in supercritical CO_2.

In contrast to $scCO_2$ and scN_2O, in $scCF_3H$, the time constant for the final decay at 545 nm was considerably reduced at higher densities. The same type of density dependence was also observed at the probe wavelength 390 nm. It is interesting that the decay process of 12′C in supercritical CF_3H was not monoexponential. For instance, a biexponential fit of the decay yielded components with time constants τ_{1A} and τ_{1B} having typical amplitude ratios between 2:1 and 3:1. We further note that such a biexponential decay for 12′C was also observed in liquid CF_3H (200 bar and 296 K). In liquids, a higher solubility of 12′C is expected, and therefore, the consistent behavior in liquid and supercritical CF_3H discards possible artifacts on the signal such as a substantial response of molecules adsorbed preferentially on the cell window surfaces. In any case, the amount of 12′C loaded into the cell was kept below the respective solubility limit under that specific condition, and the cell was homogeneously thermalized before and during the measurements.

Another interesting fact is the observation of stimulated emission signals at the probe wavelength 780 nm in $scCF_3H$ and very weakly also in $scCO_2$ (not shown here). At this probe wavelength, the evolution of the transient signals is characterized by a fast decay of a strong $S_2 \rightarrow S_n$ absorption at early times (time constant τ_2 < ca. 100−150 fs, limited by the temporal resolution of the experimental setup) followed by the formation of a stimulated emission signal (τ_3, in the range 0.3−1.0 ps), which subsequently decays on a much slower time scale (S_1/ICT $\rightarrow S_0$). Similar transients were recorded previously in organic solvents.[18] Two time constants τ_{1A} and τ_{1B} were determined for the final decay in supercritical CF_3H as in the GSB and ESA transients. In supercritical CO_2, stimulated emission was present but too weak to extract a reliable decay time constant.

The temperature dependence of lifetimes of 12′C in SCFs appeared to be insignificant; see, e.g., the values at the same density in CF_3H at 323 K/150 bar and 308 K/100 bar or at 323 K/250 bar and 308 K/175 bar, recorded at the probe wavelength 545 nm (Supporting Information Table S3 (ii)). The normalized transient absorption signals at a given CF_3H density were practically identical.

3.2.2. 8′-Apo-β-caroten-8′-al. We also investigated the ultrafast excited-state dynamics of 8′C in $scCO_2$ and $scCF_3H$ over the pressure range 85−300 bar at the temperatures 308 and 323 K. After excitation to the S_2 state at 390 nm, the intramolecular dynamics were detected at probe wavelengths located on the $S_0 \rightarrow S_2$ (390 nm) and S_1/ICT $\rightarrow S_n$ (545, 580, 600, and 650 nm) absorption bands.

Figure 6 compares representative transient absorption signals of 8′C in supercritical CF_3H obtained at the wavelengths 545 nm (A) and 390 nm (B). Different symbols indicate profiles for four different pressures in the range 85−300 bar at 323 K, and lines are fit results using a sum of two exponential functions convolved with the cross-correlation of the setup (see the Discussion). As for the 12′C species, the decay on longer time scales is due to S_1/ICT $\rightarrow S_0$ internal conversion (time constant τ_1). Interestingly, in contrast to the 12′C species, the final decay of the CF_3H signals can be well described by a monoexponential fit. The same is observed for CO_2. There appears to be a minor acceleration (1−2 ps) of the internal conversion at the highest CF_3H pressures. The temperature change from 323 to 308 K did not result in a systematic variation of τ_1. Supporting Information Table S4 summarizes all experimental conditions and the measured internal conversion time constants.

3.2.3. Polarization Spectroscopy. The internal conversion time constants in Supporting Information Tables S3 and S4 were obtained at magic angle configuration (54.7°) between the pump and probe beams. Figure 7 illustrates the outcome of additional polarization-dependent transient absorption signals of 12′C in $scCF_3H$ (P = 100 bar and T = 323 K), measured at parallel and perpendicular relative polarizations between the pump and probe beams. We further confirmed that the shape of the transient absorption signal at magic angle configuration (I_{magic}) was identical to the calculated temporal profile from the signals measured at parallel (I_{par}) and perpendicular (I_{perp}) polarizations using the expression[28]

$$I_{magic}(t) = \frac{I_{par}(t) + 2I_{perp}(t)}{3} \quad (4)$$

Table 1 contains a summary of the resulting orientational relaxation times for the S_1/ICT state, and a Stokes−Einstein−Debye plot of τ_{or} against the temperature-reduced viscosity can be found in Figure 8.

TABLE 1: Orientational Relaxation of 12′-Apo-β-caroten-12′-al (12′C) in Supercritical Fluids and Organic Solvents[a]

solvent	λ_{pump} (nm)	λ_{probe} (nm)	P (bar)	T (K)	η (cP)	η/T (10^{-3} cP/K)	τ_{or} (ps)
CO_2	390	545	100	323	0.0285	0.088	10.2
	390	545	200	323	0.0688	0.213	18.1
CF_3H	390	545	100	323	0.0515	0.159	19.4
	390	545	300	323	0.1031	0.319	28.7
n-hexane	390	545	1	298	0.3000	1.007	63.0
ethyl acetate	430	860	1	298	0.4230	1.419	71.5
i-octane	430	860	1	298	0.5080	1.705	105

[a] Solvent properties for the supercritical fluids (e.g., density and viscosity) were taken from ref 15.

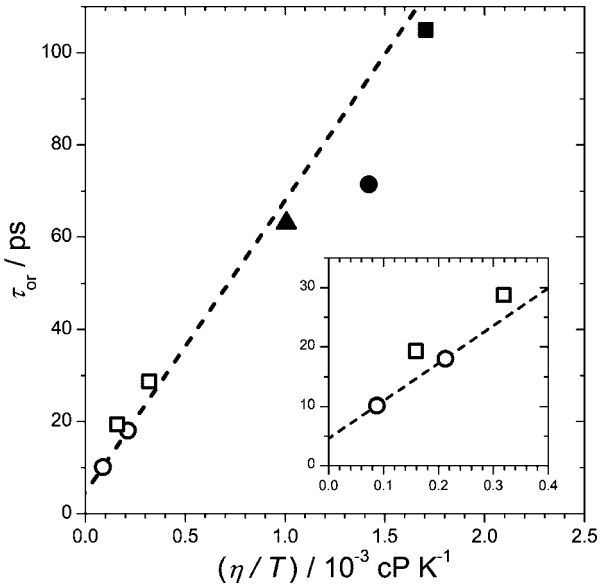

Figure 8. Stokes−Einstein−Debye plot of the orientational relaxation times τ_{or} of 12′C in various solvents. Organic solvents at 298 K: (▲) *n*-hexane; (●) ethyl acetate; (■) *i*-octane. Supercritical fluids at 323 K: (○) $scCO_2$ at 100 and 200 bar; (□) $scCF_3H$ at 100 and 300 bar. The dashed line represents a linear fit to the data in $scCO_2$ only (τ_{or} [ps] = (4.6 + 63.4(η/T) [10^{-3} cP/K])). Inset: Data in supercritical fluids at low η/T. For values, see Table 1.

4. Discussion

4.1. Steady-State Absorption Spectra. The observation of a significant hypsochromic spectral shift (ca. 20−30 nm) for both apocarotenals in supercritical fluids relative to *n*-hexane is consistent with earlier findings of C_{40} carotenoids in supercritical fluids.[5,29−32] Interestingly, with the same value $R(n)$ = 0.1, in the case of 12′C, the spectra in $scCO_2$ and in $scCF_3H$ are slightly shifted with respect to each other, whereas for 8′C both spectra almost coincide, except for a broader shape and a slight asymmetric broadening (tail) toward lower energies in the case of $scCF_3H$. A qualitatively similar behavior can also be observed in the comparison of the spectra in *n*-hexane and methanol. This indicates that, in the case of 12′C, the S_0-S_2 energy gap is not exclusively determined by the solvent polarizability, but solvent polarity becomes more influential (see below). The asymmetric broadening has been frequently attributed to the dipolar character of the electronic ground state S_0. In polar solvents, stabilization of the negative partial charge on the carbonyl oxygen possibly leads to a broader distribution of conformers and therefore a loss of vibrational structure and an additional broadening of the spectra.[33−35] The "pure" thermochromic shift of the spectra can be easily analyzed in supercritical fluids, because the density can be kept constant when varying the temperature by adjusting the pressure. We note that the thermochromic shift is rather small and its absolute size appears to be only slightly dependent on the carotenoid and the solvent.[36]

In a conventional approach, as, e.g., explored for a range of C_{40} carotenoids in our earlier experiments,[5] one can consider the correlation of the absorption peak position with the solvent polarizability $R(n)$ in order to extrapolate the energy of the $S_0 \rightarrow S_2$ transition to the gas-phase limit when $R(n) = 0$. This is rather straightforward for the data in nonpolar organic solvents and nondipolar $scCO_2$, where the clear vibronic structure permits simulating the absorption band by a sum of multiple Gaussian peaks and extracting the position of the 0−0 transition. For the C_{40} carotenoid β-carotene, where the vibronic band structure is well-resolved, we showed that the absorption peak position near 450 nm is linearly dependent on solvent polarizability, with a ca. 30 times stronger dependence on solvent polarizability than polarity.[5] Similarly, an analysis of the additional influence of solvent polarity on the extrapolation of the location of absorption maxima indicates only a minor contribution of ca. 12% for 12′C and ca. 5% for 8′C. However, the current results in Figure 4 demonstrate that such an extrapolation to the gas-phase limit is rather difficult in the case of apocarotenals: First, for 12′C and 8′C in polar solvents, it is difficult to reliably correlate the apparent absorption maximum with the $S_0 \rightarrow S_2(0-1)$ transition, because the vibronic band structure is completely washed out. Second, there are signs of solvent clustering, i.e., excess solvent density in the vicinity of the carotenoid due to attractive interactions in the compressible regime of the supercritical fluids.[12,37,38] This is particularly obvious for the absorption shifts in CO_2 and CF_3H at 308 K in Figure 4 (squares), which level off with decreasing fluid density. Measurements at lower densities were not feasible due to the low solubility and the negligible vapor pressure of the carotenoids. Further away from the critical temperature (323 K, circles), the curvature due to solvent clustering effects is weaker but still visible.

We have applied a simple spectral shift analysis to the 12′C and 8′C spectra by considering only the data in nonpolar organic solvents (298 K) and in supercritical CO_2 at 323 K (thermochromic shifts are negligible, see above). The correlation of the absorption maximum $\tilde{\nu}_{max}$ ($1^1B_u^+$) with solvent polarizability using a linear function results in the following expressions:

For 12′-apo-β-caroten-12′-al (12′C),

$$\tilde{\nu}_{max}(1^1B_u^+) = [(26547 \pm 230) - (10289 \pm 900)\cdot R(n)]\ \mathrm{cm}^{-1} \quad (5)$$

For 8′-apo-β-caroten-8′-al (8′C),

$$\tilde{\nu}_{max}(1^1B_u^+) = [(24211 \pm 30) - (9720 \pm 170)\cdot R(n)]\ \mathrm{cm}^{-1} \quad (6)$$

where the intercept in eqs 5 and 6 is the absorption maximum (0−1 vibrational transition) of the $S_0(1^1A_g^-) \rightarrow S_2(1^1B_u^+)$

electronic transition in the gas-phase limit. We obtained linear regression coefficients around 0.98. Values for the 0−0 transitions of both species were then determined by subtracting the 0−1 vibrational spacing from the intercepts in eqs 5 and 6, resulting in our final estimates of 24880 cm^{-1} (402 nm) and 22736 cm^{-1} (440 nm), respectively, for the $S_0 \rightarrow S_2(0-0)$ transition of the two apocarotenals.

Interestingly, in the case of 12′C, there is a clear difference in absorption shifts for the measurements in $scCO_2$ and $scCF_3H$ at given $R(n)$ values. Obviously, the polarity of CF_3H is responsible for the additional red shift of the $S_0 \rightarrow S_2$ transition for this apocarotenal. Both apocarotenals already possess a substantial dipole moment in the ground electronic state: our preliminary DFT calculations suggest a value of ca. 8 D for 12′C, which is expected to increase significantly upon photoexcitation to the S_2 state. For 8′C, a slightly larger value of ca. 10 D is found for the ground electronic state, which is reasonable for a longer conjugated system. The relative increase in dipole moment upon photoexcitation is obviously larger in the case of 12′C, which leads to the larger sensitivity of its $S_0 \rightarrow S_2$ transition energy to polarity. An increased influence of solvent polarity on the spectral shift of the absorption maxima for 12′C (ca. 12%) compared to 8′C (ca. 5%), which can be inferred from a bilinear fitting procedure,[5] is consistent with this viewpoint.

4.2. Transient Absorption Signals in Supercritical Fluids.

4.2.1. Solvent Dependence of τ_1 of 12′-Apo-β-caroten-12′-al. We have previously studied the polarity dependence of the IC time constant τ_1 in a range of organic solvents.[18,19] Lifetimes varied strongly between 220 ps in nonpolar solvents (*n*-hexane) and 8 ps in polar solvents (methanol). The acceleration was interpreted in terms of a successive decrease of the energy gap between the S_1/ICT and S_0 states in media of increasing polarity. A clear onset of polarity dependence was found at $\Delta f \approx 0.3$. All decays were very well described by monoexponential fits. It is interesting to compare those results with the ones obtained in the current study in SCFs in Figure 9.

For fitting the experimental data, we used the following function:

$$I(t) = \left(A_0 + A_{1A}\exp\left\{-\frac{t-t_0}{\tau_{1A}}\right\} + A_{1B}\exp\left\{-\frac{t-t_0}{\tau_{1B}}\right\} + A_3\exp\left\{-\frac{t-t_0}{\tau_3}\right\}\right)\cdot 0.5\left(1 + \mathrm{erf}\left\{\frac{t-t_0}{\sqrt{2}\sigma}\right\}\right) \quad (7)$$

Here, A_{1A}, A_{1B}, τ_{1A}, and τ_{1B} correspond to amplitudes and time constants for describing the final decay of the transient signal, which is related to the S_1/ICT $\rightarrow S_0$ transition of central interest in this paper. The third exponential (A_3, τ_3) describes the "round shape" observed in the ESA (vis) and stimulated emission (near IR) responses of carbonyl carotenoids at early times, which is tentatively ascribed to "ICT formation" (values found in the current work are in good agreement with those found previously in organic solvents).[18,26,27,39] A_0 accounts for very small offsets in some of the transients. t_0 enables slight adjustments of time zero in the fit, and the error function term accounts for the finite time resolution of the setup characterized by the cross-correlation σ. Note that for the sake of simplicity and better convergence of the fit we do not use a separate time constant to describe the ultrafast $S_2 \rightarrow S_1$/ICT step (literature values are around 160 fs or less),[40] because it is in the range of the cross-correlation and can be well described by an effective σ.

In the case of $scCO_2$, the S_1/ICT $\rightarrow S_0$ step was well described by a monoexponential decay ($A_1 = A_{1A}$, $\tau_1 = \tau_{1A}$, and $A_{1B} = 0$ in eq 7), and the τ_1 values showed no systematic pressure dependence in the pressure range employed (Figure 5A), regardless of probe wavelength. Averaged time constants of 197 and 186 ps were obtained at the two wavelengths. Similarly, no clear systematic variations of τ_1 were found when changing to scN_2O, and a comparable average decay time was obtained (187 ps). Interestingly, in $scCO_2$, the internal conversion appears to be slightly faster than expected on the basis of the Δf values alone (Figure 9), which would suggest a value >205 ps for nonpolar solvents in this Δf range. It is reasonable to assume that the substantial quadrupole moment of "nondipolar"[16] CO_2 could result in a sufficient stabilization of the S_1/ICT state relative to S_0, which slightly accelerates internal conversion. No Δf values are unfortunately available in the case of N_2O. Here, the weak dipole moment of N_2O (0.16 D)[41] might be responsible for the faster internal conversion compared to nonpolar solvents.

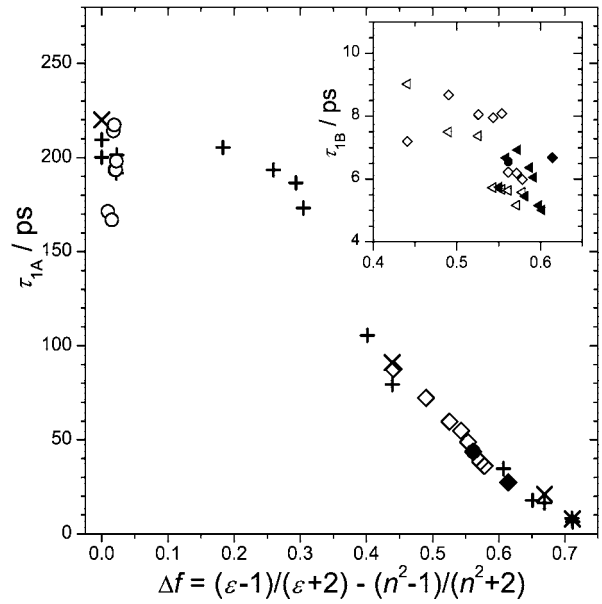

Figure 9. Time constants τ_{1A} and τ_{1B} for 12′C in various solvents as a function of the solvent polarity function Δf (see Supporting Information Table S3). Main figure (τ_{1A} values): (×) Transient absorption experiments in *n*-hexane, tetrahydrofuran, ethanol, and methanol at 298 K in increasing order of solvent polarity from ref 19; (+) transient stimulated emission results from ref 18 at 298 K; transient absorption experiments from this work in $scCO_2$ at 323 K (○), in $scCF_3H$ at 323 K (◇), and in liquid CF_3H at 296 K (◆) using $\lambda_{pump} = 390$ nm and $\lambda_{probe} = 390$ nm. (●) Transient stimulated emission experiment in $scCF_3H$ at 323 K with $\lambda_{pump} = 390$ nm and $\lambda_{probe} = 780$ nm. Data at the probe wavelength 545 nm in supercritical fluids are very similar to those measured at $\lambda_{probe} = 390$ nm and therefore not shown here for the sake of clarity. The inset shows τ_{1B} values from this work in $scCF_3H$: The symbols ◇, ◆, and ● are the same as those above; the solid and open left-pointing triangles are the measurements with $\lambda_{pump} = 390$ nm and $\lambda_{probe} = 545$ nm at the temperatures 323 and 308 K, respectively.

In contrast to $scCO_2$ and scN_2O, a significant pressure dependence of the lifetime was observed in polar $scCF_3H$ (Figure 5B). This is not unexpected because a density increase progressively increases Δf, in the current work covering the range 0.44−0.61 (Supporting Information Table S3). The most surprising result, however, is that the decays in CF_3H are clearly not monoexponential, in contrast to the organic solvents investigated previously.[18,19] The decays at all densities can be well described by biexponential fits with the time constants τ_{1A} and τ_{1B} and the amplitudes A_{1A} and A_{1B} given in Supporting Information Table S3. Interestingly, the density dependence of

τ_{1A} fits well into the almost linear correlation for this Δf range previously established in a range of organic solvents (26−88 ps, see diamond symbols in Figure 9). The second component relaxes much faster (τ_{1B} in the range 5−9 ps, see the inset in Figure 9). We also note that the GSB, ESA, and SE profiles all show biexponential decay characteristics.

We consider the following possible scenarios:

(1) The decays could be sensitive to the time-dependent solvation of the highly polar S_1/ICT state. Measurements of solvation times under approximately the conditions studied in this paper, show time constants in the 3−10 ps range,[6] comparable to the fast time component (5−9 ps) observed here.

(2) Processes such as vibrational relaxation or relaxation of conformationally unrelaxed intermediates within a single electronic state could affect the transients and lead to the observed biexponential behavior. For instance, a blue shift of the S_1/ICT band with a time constant of 5−9 ps (corresponding to the fast time constant observed in the transients) could be responsible for the initial fast decay of the S_1/ICT transient absorption and the fast "refill" of the ground-state bleach.

(3) It could be that two separate parallel channels for population transfer between the excited and ground electronic states are present. These could be two independent channels originating from the same electronic state, which do not "communicate" with each other or are connected by an equilibrium having negligibly slow forward and backward rates for interconversion. Alternatively, there could be even two different separate electronic states which decay independently and have similar excited-state absorption spectra. It is, however, difficult to rationalize why in none of the organic solvents in this Δf range studied previously such a deviation from monoexponential behavior has been observed.[18,19]

(4) The formation of small clusters or aggregates of apocarotenals could lead to excitonic interactions after photoexcitation, resulting, e.g., in exciton−exciton annihilation processes. It was demonstrated that large zeaxanthin aggregates exhibit multiexponential decays with decay components faster than the S_1 lifetime.[42] However, such carotenoid aggregates of H- or J-type should exhibit characteristic changes in the steady-state absorption spectra,[43,44] which were, however, not observed in the current study. In addition, apocarotenal concentrations were kept below the solubility limit in the respective SCF, which should minimize aggregation. The deviation from monoexponential behavior for the 12′C species even in liquid CF_3H also suggests that aggregate formation is highly likely to not be responsible for the observed deviation from single exponential behavior.

(5) Specific solvation effects of the supercritical CF_3H could also be involved. The SCF could provide a variety of heterogeneous microenvironments for the carotenoid molecules (specific "carotenoid−$(CF_3H)_n$ cluster conformers"), which relax on different time scales. The biexponential fit parameters in Supporting Information Table S3 could be interpreted in a way that there might be two types of populations:[45] one with a homogeneous solvation structure around the carotenoid, resulting in decay time constants expected for a normal liquid with the respective Δf, and another one with more "efficient", possibly asymmetric preferential solvation of the negative carbonyl oxygen, considerably stabilizing the S_1/ICT state to an extent which is comparable to the stabilization in methanol or acetonitrile. It is, however, very unlikely at the high temperatures and densities studied here that such clusters would persist long enough to result in such heterogeneous dynamics.

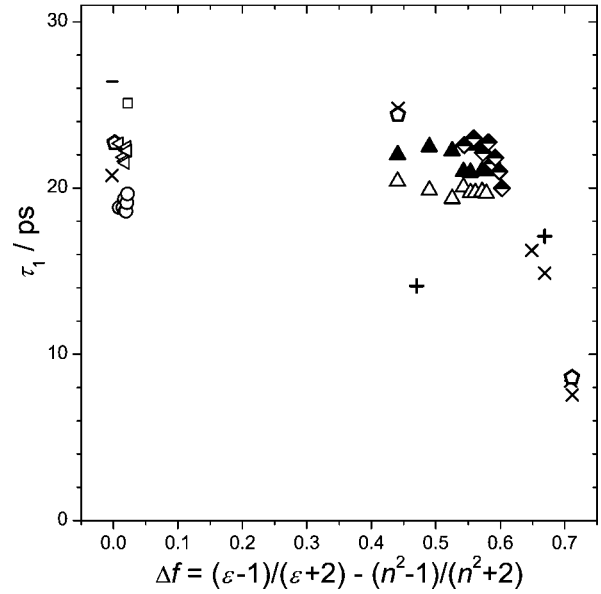

Figure 10. Internal conversion time constants τ_1 of 8′C in various solvents as a function of the solvent polarity function Δf (see Supporting Information Table S4). Transient absorption experiments in liquids at 298 K from refs 53 (□), 54 (−), 55 (+), and 17 (⌂). Transient stimulated emission results from ref 18 (×). Transient absorption experiments in supercritical fluids (this work): $\lambda_{pump} = 390$ nm and $\lambda_{probe} = 545$ nm: in $scCO_2$ at 323 K (left-pointing triangles), in $scCF_3H$ at 323 K (▲) and 308 K (partially solid and open diamonds); $\lambda_{pump} = 390$ nm and $\lambda_{probe} = 390$ nm: in $scCO_2$ at 323 K (○), in $scCF_3H$ at 323 K (△).

Clustering effects might be, however, relevant to the steady-state absorption spectra discussed in section 4.1. In that case, a leveling-off of the spectral shifts was observed for the $S_0 \rightarrow S_2$ transition, indicating a significant increase of the local density around the solute relative to the average density of the supercritical fluid. A substantial increase of the dipole moment of the carotenoid upon transition to the S_1/ICT state combined with considerable van der Waals attraction of this large organic molecule might be an important prerequisite for the operation of such specific effects. It is unclear at the moment, though, how exactly the solvent molecules are distributed around the solute at different SCF densities and temperatures. MD simulations will be useful in this respect, and are currently underway in our groups. In any case, the departure from monoexponential behavior observed in CF_3H—even in the liquid—is puzzling, and additional experimental work, e.g., involving pump−supercontinuum probe (PSCP) broadband absorption techniques[40,46] at different pump wavelengths will be needed to clarify the dynamics.

4.2.2. Solvent Dependence of τ_1 of 8′-Apo-β-caroten-8′-al. In organic solvents, 8′C, which has a longer conjugation length, is known to exhibit a less pronounced polarity dependence of its S_1/ICT lifetime than 12′C. Values vary between 25 ps in *i*-octane and 8 ps in methanol. Also, the polarity dependence appears only at higher polarities ($\Delta f > 0.6$).[17,18] Figure 10 contains our measured S_1/ICT $\rightarrow S_0$ internal conversion time constants τ_1 for 8′C as a function of solvent polarity, including the present data in supercritical fluids. The solvent polarity in SCFs was varied by the change of pressure and temperature over the range $\Delta f = 0.01-0.02$ in $scCO_2$ and $0.44-0.60$ in $scCF_3H$. Almost identical S_1/ICT $\rightarrow S_0$ internal conversion time constants τ_1 of 8′C were obtained on variation of the solvent polarity in the range $\Delta f = 0.01-0.60$. The same observation has been made in both $scCO_2$ and $scCF_3H$. An average τ_1 value of 20.6 ps in CO_2 and 21.1 ps in CF_3H was

determined. At the highest Δf values reached in this work in $scCF_3H$ at 308 K (0.58−0.60), a slight reduction of τ_1 values can be recognized. This observation is consistent with the onset of polarity dependence in this Δf region previously measured in organic solvents.[17,18] Obviously, there is a characteristic difference regarding the onset and the strength of the solvent dependence of τ_1 between the two apocarotenals. In this respect, especially the new data in CF_3H enable us to locate the onset of the solvent polarity dependence of τ_1 for 8′C more precisely.

Interestingly, the decay of the S_1/ICT state of 8′C in CF_3H can be described by a monoexponential function, whereas it was clearly biexponential (or stretched-exponential) for the 12′C species. We note, however, at this point that a biexponential representation including a fast component with smaller amplitude can also fit the data in a satisfactory way. To select only one specific example in $scCF_3H$ (308 K, 300 bar, $\lambda_{probe} = 545$ nm), an acceptable fit to the experimental data is possible using the parameters $\tau_{1A} = 24$ ps, $A_{1A} = 60\%$, $\tau_{1B} = 5$ ps, $A_{1B} = 20\%$, $\tau_3 = 1.0$ ps, and $A_3 = -20\%$. In other words, due to the fact that the two time constants in the biexponential fit are not as different as in the case of the 12′C species, it might well be that there is an additional fast component hidden in the signals. Possibly the 12′C species represents a "lucky case" where the time constants are different enough to be separable.

4.2.3. Orientational Relaxation in Supercritical Fluids. In Figure 7 (inset), an example for a resulting anisotropy function $r(t)$ of 12′C in $scCF_3H$ is shown. It can be obtained from polarization spectroscopy via

$$r(t) = \frac{I_{par}(t) - I_{perp}(t)}{I_{par}(t) + 2I_{perp}(t)} \tag{8}$$

To a very good approximation, carotenoids can be treated as symmetric prolate tops, i.e., $A \approx B < C$ for the rotational constants. We have carried out preliminary DFT calculations for 12′C using the Gaussian 03 program package[47] at the B3LYP/6-31G(d,p) level. The minimum energy structure is of *s-cis* type, where the β-ionone ring adopts an out-of-plane configuration with a C5═C6−C7═C8 dihedral angle (Figure 1) of ca. 46° relative to the *all-trans* polyene backbone. The resulting rotational constants for the ground electronic state are $A = 0.0348740$, $B = 0.0360767$, and $C = 0.5676433$ GHz, and should be good approximations for the rotational constants of the S_1/ICT state, in which the orientational relaxation occurs. Additional preliminary calculations by us employing TDDFT suggest that the pump and probe transition dipole moments lie almost parallel to the figure axis of the carotenoid ($\pi-\pi^*$ transitions involving the polyene system). In such a case, the following simple expression can be used for $r(t)$:

$$r(t) = 0.4 \exp(-\tau_{or}t) = 0.4 \exp(-6D_{perp}t) \tag{9}$$

Here, τ_{or} denotes the orientational relaxation (or rotational relaxation) time, and D_{perp} is the rotational diffusion constant for the rotation around the inertial axes perpendicular to the figure axis. Therefore, the anisotropy can reach a limiting value of 0.4 at $t = 0$. The line in the inset of Figure 7 represents the best monoexponential fit to $r(t)$, from which an orientational relaxation time τ_{or} of 28.7 ps is determined under these conditions ($scCF_3H$, $T = 323$ K, $P = 300$ bar). Extrapolation toward $t = 0$ yields $r(0) = 0.32$, which is slightly smaller but still close to the limiting value of 0.4 implied by eq 9. We also note that a value of 0.34 for the initial anisotropy is obtained at the probe wavelength 860 nm in our measurements in *i*-octane, which is probing an $S_2 \rightarrow S_n$ transition at early times. Possible reasons for the smaller values in both cases could be, e.g., a slight difference in the direction of the pump and probe transition dipole moments for the respective transitions and/or the presence of a very fast inertial component of orientational relaxation, which is hidden in the noise of the anisotropy curve around $t = 0$. Deviations due to pressure-induced birefringence of the sapphire windows can be neglected at the relatively low pressures employed in the current study.[48]

We have carried out polarization-dependent measurements under different experimental conditions, such as different supercritical fluids ($scCO_2$ or $scCF_3H$) at different densities. Table 1 contains a summary of the orientational relaxation times determined from these measurements, as well as comparative measurements by us in three organic solvents. τ_{or} increases with increasing shear viscosity of the solvent. Such a behavior is frequently described in the framework of hydrodynamic models of the Stokes−Einstein−Debye (SED) type.[4,49,50] The modified SED equation is given as

$$\tau_{or} = \frac{V_h \eta}{k_B T} fC + \tau_0 \tag{10}$$

Here, V_h is the hydrodynamic volume of the molecule, η the viscosity of the medium, and T the temperature. f is a variable parameter depending on molecular shape, C is a dimensionless parameter which accounts for boundary conditions associated with the free volume effect (interaction of the dissolved molecule with the surrounding medium),[51] and τ_0 is the free rotor time. In the case of SED behavior, τ_{or} should be proportional to the bulk shear viscosity, and a plot of τ_{or} vs η/T should yield a straight line. Figure 8 shows such an SED plot of our data for 12′C in supercritical CO_2 and CF_3H, including complementary data in three liquids (*n*-hexane, ethyl acetate, and *i*-octane). In general, τ_{or} increases with viscosity in qualitative agreement with the SED model.

The free rotor time can be conveniently obtained by extrapolating the values in $scCO_2$ to zero viscosity. Here, we use only the values in nondipolar CO_2, because in polar solvents such extrapolations tend to yield larger values due to additional dielectric friction exerted by the solvent.[22,48] This is also implied by the CF_3H data in Figure 8, which would result in a value of 10.1 ps for the intercept. From the extrapolation of the CO_2 data, we obtain $\tau_0 = 4.6$ ps for the free rotor time of 12′C. This value is in very good agreement with the calculated free rotor time of 5.2 ps, which was determined using our calculated rotational constants and the expression recommended by Bartoli and Litovitz:[52]

$$\tau_0 = 2\pi \frac{41}{360} \sqrt{\frac{I_{eff}}{k_B T}} \tag{11}$$

where I_{eff} is calculated as the harmonic mean of the two inertial moments for the A and B principal axes:

$$I_{eff} = \frac{h}{4\pi^2 (A + B)} \tag{12}$$

This favorable agreement is not surprising for such a large organic molecule rotating in a fluid consisting of relatively small

nondipolar solvent molecules, which should minimize "slip" effects which, e.g., occur for small solute molecules rotating relatively "freely" in the voids of a fluid consisting of large solvent molecules.[22] The value of 4.6 ps for 12′C is in line with results for smaller molecules such as *p*-terphenyl (2.6 ps), *trans*-stilbene (2.0 ps), *N*,*N*-diethylaniline (1.7 ps), and biphenyl (1.6 ps) from earlier work.[22]

It can be clearly seen in Figure 8 that the τ_{or} values of 12′C in various liquids (*n*-hexane, ethyl acetate, and *i*-octane) deviate from the extrapolation of τ_{or} values based on the data in CO_2. This is, however, not surprising, because variations of the type of solvent not only change viscosity but also the size ratio between the solute and solvent molecules as well as the interactions of the solvent with the solute. SCFs have decisive advantages in this respect: (1) Density can be changed without changing chemical identity. (2) Viscosities much lower than those in standard organic solvents can be reached. (3) The size of the CO_2 fluid molecules is relatively small, especially compared to the large solute species studied in this paper, which makes hydrodynamic theories better applicable.

5. Conclusions

We provided a comprehensive experimental investigation of the excited-state dynamics of two carbonyl containing apocarotenoids, 12′-apo-β-caroten-12′-al (12′C) and 8′-apo-β-caroten-8′-al (8′C), in supercritical CO_2, CF_3H, and N_2O over the pressure range 85−300 bar and at the temperatures 308 and 323 K. The presence of ICT character in the lowest excited electronic state was confirmed by its characteristic near IR stimulated emission observed in $scCO_2$ and $scCF_3H$. The strong polarity dependence of the lifetime of the S_1/ICT state previously found in organic solvents[17−19] was also observed in SCFs when varying the polarity of CF_3H by density tuning. Two new observations deserve attention: First, transient absorption profiles for 12′C in CF_3H suggested that the S_1/ICT state in this solvent did not decay in a simple single exponential fashion. Second, the solvent shifts of the steady-state absorption spectra of the apocarotenals in SCFs displayed pronounced saturation effects with decreasing density. The nonexponential decay could be due to time-dependent solvation of the S_1/ICT state, vibrational cooling, or conformational relaxation processes of 12′C. The solvent shifts could indicate that solvent clustering effects[11,12] occur at the lowest pressures.

Additional experiments will be helpful, e.g., employing broadband pump−supercontinuum probe (PSCP) transient absorption spectroscopy, to evaluate the full spectral dynamics from the UV/vis to the near IR region. In addition, we are currently carrying out MD simulations to investigate if there are specific differences in the microscopic solvation structure of the apocarotenals in SCFs and organic solvents. Finally, anisotropy decays of 12′C in different solvents provided orientational relaxation time constants which were approximately proportional to viscosity. The values for $scCO_2$ taken in the low-vicosity regime were extrapolated to zero viscosity and provided a free rotor time close to the value calculated on the basis of the rotational constants, in reasonable agreement with simple hydrodynamic models.

Acknowledgment. Financial support from the Alexander von Humboldt foundation in the framework of the Sofja Kovalevskaja program and the German Science Foundation and helpful discussions with V. G. Ushakov, D. A. Wild, D. Tuma, and J. Gierschner as well as generous experimental support from R. Bürsing are gratefully acknowledged. Some of the steady-state absorption spectra were provided by Z. Chen and J. Seehusen. We are particularly thankful to the BASF AG, and here especially H. Ernst, for providing the highly purified *all-trans*-apocarotenal samples and extensive advice. We would also like to thank the reviewers for very helpful suggestions, especially regarding the interpretation of the transient absorption decays of 12′C in CF_3H.

Supporting Information Available: Table S1: Absorption maxima of 12′-apo-β-caroten-12′-al (12′C) in various solvents. Table S2: Absorption maxima of 8′-apo-β-caroten-8′-al (8′C) in various solvents. Table S3: Lifetimes of 12′-apo-β-caroten-12′-al (12′C) in supercritical fluids. Table S4: Lifetimes of 8′-apo-β-caroten-8′-al (8′C) in supercritical CO_2 and CF_3H. Figure S1: Density-dependent steady-state absorption spectra of 12′-apo-β-caroten-12′-al (12′C) in supercritical fluids. Figure S2: Density-dependent steady-state absorption spectra of 8′-apo-β-caroten-8′-al (8′C) in supercritical fluids. This material is available free of charge via the Internet at http://pubs.acs.org.

References and Notes

(1) Polívka, T.; Sundström, V. *Chem. Rev.* **2004**, *104*, 2021.
(2) *The Photochemistry of Carotenoids*; Frank, H. A., Young, A. J., Britton, G., Cogdell, R. J., Eds.; Kluwer: Dordrecht, The Netherlands, 1999; Vol. 8, p 399.
(3) Arai, Y.; Sako, T.; Takebayashi, Y. *Supercritical Fluids - Molecular Interactions, Physical Properties, and New Applications*; Springer: Berlin, Heidelberg, 2002.
(4) Bürsing, R.; Lenzer, T.; Oum, K. *Chem. Phys.* **2007**, *331*, 403.
(5) Chen, Z.; Lee, C.; Lenzer, T.; Oum, K. *J. Phys. Chem. A* **2006**, *110*, 11291.
(6) Kometani, N.; Arzhantsev, S.; Maroncelli, M. *J. Phys. Chem. A* **2006**, *110*, 3405.
(7) Lee, C.; Luther, K.; Oum, K.; Troe, J. *J. Phys. Chem. A* **2006**, *110*, 2613.
(8) Luther, K.; Oum, K.; Sekiguchi, K.; Troe, J. *Phys. Chem. Chem. Phys.* **2004**, *6*, 4133.
(9) Oum, K.; Sekiguchi, K.; Luther, K.; Troe, J. *Phys. Chem. Chem. Phys.* **2003**, *5*, 2931.
(10) Oum, K.; Harrison, J. J.; Lee, C.; Wild, D. A.; Luther, K.; Lenzer, T. *Phys. Chem. Chem. Phys.* **2003**, *5*, 5467.
(11) Lewis, J. E.; Biswas, R.; Robinson, A. G.; Maroncelli, M. *J. Phys. Chem. A* **2001**, *105*, 3306.
(12) Schwarzer, D.; Troe, J.; Zerezke, M. *J. Chem. Phys.* **1997**, *107*, 8380.
(13) Sun, Y. P. *Supercritical Fluid Technology in Materials Science and Engineering*; Marcel Dekker, Inc.: New York, 2002.
(14) Kajimoto, O. *Chem. Rev.* **1999**, *99*, 355.
(15) http://webbook.nist.gov, 2008.
(16) Raveendran, P.; Ikushima, Y.; Wallen, S. L. *Acc. Chem. Res.* **2005**, *38*, 478.
(17) Ehlers, F.; Wild, D. A; Lenzer, T.; Oum, K. *J. Phys. Chem. A* **2007**, *111*, 2257.
(18) Kopczynski, M.; Ehlers, F.; Lenzer, T.; Oum, K. *J. Phys. Chem. A* **2007**, *111*, 5370.
(19) Wild, D. A.; Winkler, K.; Stalke, S.; Oum, K.; Lenzer, T. *Phys. Chem. Chem. Phys.* **2006**, *8*, 2499.
(20) Ricci, M.; Torre, R.; Foggi, P.; Kamalov, V.; Righini, R. *J. Chem. Phys.* **1995**, *102*, 9537.
(21) Foggi, P.; Righini, R.; Torre, R.; Kamalov, V. F. *Chem. Phys. Lett.* **1992**, *193*, 23.
(22) Benzler, J. Ph.D. Thesis, University of Göttingen, 1997.
(23) Stalke, S.; Wild, D. A.; Lenzer, T.; Kopczynski, M.; Lohse, P. W.; Oum, K. *Phys. Chem. Chem. Phys.* **2008**, *10*, 2180.
(24) Semikolenov, S. V.; Dubkov, K. A.; Starokon, E. V.; Babushkin, D. E.; Panov, G. I. *Russ. Chem. Bull.* **2005**, *54*, 948.
(25) Mordi, R. C.; Walton, J. C.; Burton, G. W.; Hughes, L.; Ingold, K. U.; Lindsay, D. A.; Moffatt, D. J. *Tetrahedron* **1993**, *49*, 911.
(26) Zigmantas, D.; Polívka, T.; Hiller, R. G.; Yartsev, A.; Sundström, V. *J. Phys. Chem. A* **2001**, *105*, 10296.
(27) Lohse, P. W.; Bürsing, R.; Lenzer, T.; Oum, K. *J. Phys. Chem. B* **2008**, *112*, 3048.
(28) For this, a minor rescaling of the relative signal amplitudes of the measurements at parallel and perpendicular configurations was necessary, due to slightly different experimental conditions, i.e., overlap of the two beams as well as pulse energies when rotating the polarizer.

(29) Tuma, D.; Schneider, G. M. *Fluid Phase Equilib.* **1999**, *158*−*160*, 743.

(30) Tuma, D. Ph.D. Thesis, Ruhr University Bochum, 1999.

(31) Hui, B.; Young, A. J.; Booth, L. A.; Britton, G.; Evershed, R. P.; Bilton, R. F. *Chromatographia* **1994**, *39*, 549.

(32) Jay, A. J.; Steytler, D. C. *J. Supercrit. Fluids* **1992**, *5*, 274.

(33) Frank, H. A.; Bautista, J. A.; Josue, J.; Pendon, Z.; Hiller, R. G.; Sharples, F. P.; Gosztola, D.; Wasielewski, M. R. *J. Phys. Chem. B* **2000**, *104*, 4569.

(34) Shima, S.; Ilagan, R. P.; Gillespie, N.; Sommer, B. J.; Hiller, R. G.; Sharples, F. P.; Frank, H. A.; Birge, R. R. *J. Phys. Chem. A* **2003**, *107*, 8052.

(35) Zigmantas, D.; Hiller, R. G.; Yartsev, A.; Sundström, V.; Polívka, T. *J. Phys. Chem. B* **2003**, *107*, 5339.

(36) For 12′C in $scCO_2$, the change of temperature over 308−332 K at constant density (reduced density $\rho_r = \rho/\rho_c = 1.36$) resulted in a small shift of 164 cm^{-1} (−2.5 nm) (see Supporting Information Table S1 (e)). Almost no thermochromic shift was observed for 12′C in $scCF_3H$ over the temperature range 308−333 K at constant density ($\rho_r = 1.70$, see Supporting Information Table S1 (h)). In the case of 8′C, thermochromic shifts of 224 cm^{-1} (−4.1 nm) in $scCO_2$ over the temperature range 309−333 K at the constant density $\rho_r = 1.29$ (see Supporting Information Table S2 (e)) and of 220 cm^{-1} (−4.2 nm) in $scCF_3H$ at the constant density $\rho_r = 1.70$ over the temperature range 308−334 K (see Supporting Information Table S2 (h)) were observed.

(37) Patel, N.; Biswas, R.; Maroncelli, M. *J. Phys. Chem. B* **2002**, *106*, 7096.

(38) Song, W.; Biswas, R.; Maroncelli, M. *J. Phys. Chem. A* **2000**, *104*, 6924.

(39) Zigmantas, D.; Hiller, R. G.; Sharples, F. P.; Frank, H. A.; Sundström, V.; Polívka, T. *Phys. Chem. Chem. Phys.* **2004**, *6*, 3009.

(40) Pérez Lustres, J. L.; Dobryakov, A. L.; Holzwarth, A.; Veiga, M. *Angew. Chem., Int. Ed.* **2007**, *46*, 3758.

(41) Reinartz, J. M. L. J.; Meerts, W. L.; Dymanus, A. *Chem. Phys.* **1978**, *31*, 19.

(42) Billsten, H. H.; Sundström, V.; Polívka, T. *J. Phys. Chem. A* **2005**, *109*, 1521.

(43) Buchwald, M.; Jencks, W. P. *Biochemistry* **1968**, *7*, 834.

(44) Simonyi, M.; Bikadi, Z.; Zsila, F.; Deli, J. *Chirality* **2003**, *15*, 680.

(45) A separation into two distinct populations might appear artificial from a physical standpoint and partly stems from the suggestive nature of the biexponential fit of the decay. We note that the decay of the transient absorption profiles in CF_3H could also be well described by using a "stretched-exponential" term instead of the first two exponential terms in eq 7, leading to $I(t) = (A_0 + A_1 \exp\{-[(t - t_0)/\tau_1]^Y\} + A_3 \exp\{-(t - t_0)/\tau_3\})\cdot 0.5(1 + \mathrm{erf}\{(t - t_0)/(\sqrt{2}\sigma)\})$. Here, the parameter Y (<1) in the first term merely describes the departure from monoexponential behavior. Such an approach (requiring one parameter less than eq 7) has been frequently used in the absence of a theoretical model to describe the relaxation of solute molecules, which are sampling different types of microenvironments within a solvent [Arzhantsev et al. *J. Phys. Chem. B* **2007**, *111*, 4978; Ingram et al. *J. Phys. Chem. B* **2003**, *107*, 5926]. Using the equation above, one obtains, e.g., in $scCF_3H$ at 308 K ($\lambda_{probe} = 545$ nm) at 90 bar, $\tau_1 = 29.9$ ps, $A_1 = 83\%$, $Y = 0.651$, $\tau_3 = 1.0$ ps, and $A_3 = -17\%$, and at 300 bar, $\tau_1 = 13.5$ ps, $A_1 = 72\%$, $Y = 0.674$, $\tau_3 = 0.6$ ps, and $A_3 = -28\%$ (compare the values in Supporting Information Table S3). Note that the parameter Y describing the stretched-exponential character of the relaxation is very similar at both pressures, emphasizing that only the overall time scale of the relaxation but not its character is changing.

(46) Kovalenko, S. A.; Dobryakov, A. L.; Ruthmann, J.; Ernsting, N. P. *Phys. Rev. A* **1999**, *59*, 2369.

(47) Frisch, M. J.; Trucks, G. W.; Schlegel, H. B.; Scuseria, G. E.; et al. *Gaussian 03*, revision B.03; Gaussian Inc.: Pittsburgh, PA, 2003.

(48) Schwarzer, D. Ph.D. Thesis, University of Göttingen, 1989.

(49) Kiyohara, K.; Kimura, Y.; Takebayashi, Y.; Hirota, N.; Ohta, K. *J. Chem. Phys.* **2002**, *117*, 9867.

(50) Bartolini, P.; Ricci, M.; Torre, R.; Righini, R.; Sánta, I. *J. Chem. Phys.* **1999**, *110*, 8653.

(51) Lee, M.; Bain, A. J.; McCarthy, P. J.; Han, C. H.; Haseltine, J. N.; Smith III, A. B.; Hochstrasser, R. M. *J. Chem. Phys.* **1986**, *85*, 4341.

(52) Bartoli, F. J.; Litovitz, T. A. *J. Chem. Phys.* **1972**, *56*, 413.

(53) Wasielewski, M. R.; Kispert, L. D. *Chem. Phys. Lett.* **1986**, *128*, 238.

(54) He, Z.; Kispert, L. D.; Metzger, R. M.; Gosztola, D.; Wasielewski, M. R. *J. Phys. Chem. B* **2000**, *104*, 6302.

(55) He, Z.; Gosztola, D.; Deng, Y.; Gao, G.; Wasielewski, M. R.; Kispert, L. D. *J. Phys. Chem. B* **2000**, *104*, 6668.

JP807086N